Theoretical analysis of the formation of membrane microtubes on axially strained vesicles

Bojan Božič,[1] Saša Svetina,[1,2] and Boštjan Žekš[1,2]
[1]*Institute of Biophysics, Medical Faculty, Lipičeva 2, SI-1105 Ljubljana, Slovenia*
[2]*J. Stefan Institute, Jamova 39, SI-1111 Ljubljana, Slovenia*
(Received 29 May 1996; revised manuscript received 10 December 1996)

The formation of membrane microtubes (tethers) was analyzed by a theoretical study of the shape changes of an axisymmetrical phospholipid vesicle caused by a pulling axial force applied at the vesicle poles. Equilibrium vesicle shapes were obtained by variationally seeking the minimum of the sum of membrane local and nonlocal bending energies at constant vesicle volume, membrane area, and the distance between the vesicle poles. The effect of axial force on vesicle shapes was studied by examining the shape behavior of prolate axisymmetrical vesicles with equatorial mirror symmetry. For a vesicle with a given relative volume, the resulting shapes reside within a given region of the phase diagram for this vesicle as a function of the distance between vesicle poles and the relative difference between the areas of the membrane layers. The upper limit of this region was obtained by a variational procedure for the determination of vesicle shapes that correspond, at given vesicle volume, membrane area, and difference between the areas of membrane layers, to the maximum distance between the vesicle poles. It was shown that for finite values of the ratio between the nonlocal and local bending moduli, at high enough axial force the vesicle shape exhibits an elongated tubular ending at each pole. The equation for the radius of such a tubular ending obtained by the rigorous treatment presented matches the equation that has previously been used as an approximation in analyses of tether formation methods for the determination of membrane bending moduli. Furthermore, it is predicted that below a certain critical value of the ratio between the two bending moduli that depends on the vesicle volume, the shape characterized by the tubular endings is attained, with continuously increasing the axial force, by a discontinuous shape transformation. [S1063-651X(97)05105-2]

PACS number(s): 87.22.Bt, 82.70.−y, 02.60.Lj

I. INTRODUCTION

Membrane microtubes, known also as tethers, are relatively long cylindrical extensions of membranes of vesicles and cells. They are frequently observed as intracellular microtubule-associated membraneous tubular organelles [1]. A tubulovesicular network can be formed by membrane associated motors moving upon microtubules [2], or a tether can be extracted from neuronal growth cones by applying an external force [3]. External forces were also shown to cause the formation of tethers from membranes of red blood cells when these, after being adhered to a glass slide, are subjected to an overflow of liquid [4]. Tethers pulled out of a red blood cell membrane do not contain a membrane skeleton and are deficient in at least some integral membrane proteins [5]. Tethers were also extracted from phospholipid vesicles [6], which indicates that their formation could be understood on the basis of the properties of phospholipid membranes.

The problem of tether extraction from vesicles can be viewed as a specific case of the problem of the formation of the vesicle shape. The above examples suggest that we are dealing with the shape of the vesicle when it is strained by an external force acting at a point. The shapes of phospholipid vesicles are governed by the elastic properties of the closed phospholipid membrane [7,8], and in this respect tethers were found to represent a suitable experimental system for studying membrane material properties [9]. They can be conveniently used for the determination of both local and nonlocal membrane bending constants, particularly since, because of their small radius, the effects of bending are much more pronounced in tethers than in rounded vesicles [10]. Tethers were recently used also for the determination of interlayer friction [11].

The aim of this work is to contribute by a rigorous theoretical treatment to the general understanding of the way in which the application of a point force on a vesicle affects its shape, with particular emphasis on revealing the conditions when such a force causes the formation of a tether, i.e., a membrane microtube. Since the usual basis for analyzing tether behavior in the determination of membrane viscoelastic constants is to estimate the elastic energy of the vesicle involving the tether by describing the system by a simple geometrical model for which the energies of different parts of the vesicle can be easily calculated [12], the present rigorous theoretical treatment also represents the necessary basis for justification of these approximate models and for defining the limits of their possible applications. Moreover, the treatment of vesicles under the influence of external forces in general represents a non-trivial generalization of the approaches that were developed in the past for the determination of the shapes of freely suspended vesicles [13]. The case of a vesicle strained by an axial force was hitherto not considered in detail. It has been shown [14] that the Euler equations that are obtained by the applying the variational principle to the problem of the shape of a vesicle strained by an axial force are identical to the Euler equations derived for an axisymmetrical vesicle [15] from the general shape equation [16]. Possible solutions of the general shape equation and their characterization represent a currently developing research interest [17]. In this respect the present work contributes in describing some examples of these solutions for axisymmetrical vesicles of spherical topology. The analysis

presented also forms the proper basis for an understanding of the formation of vesicle shapes that were observed in experiments on vesicles containing microtubule assemblies elongating along the vesicle axis and thus exerting force on its poles [18].

In this article the relevant contributions to the membrane elastic energy are presented first. Then the theoretical procedure is described for the determination of axisymmetrical shapes of bilayer vesicles under the effect of the axial force, with special emphasis on the behavior of the vesicle at its poles. It is then shown separately how to determine vesicle shapes with maximal length at a given vesicle volume, membrane area, and difference between the areas of membrane layers. The theory is used to analyze the behavior of the class of axisymmetrical prolate cigarlike shapes involving equatorial mirror symmetry.

II. DETERMINATION OF STATIONARY SHAPES OF AXIALLY STRAINED VESICLES

It is commonly believed that the shape of a vesicle or a simple cell such as an erythrocyte is determined by the minimum of the elastic energy of the membrane. We analyze the shape of a phospholipid vesicle under the assumption that the membrane area (A) does not change. Thus the elastic energy of a closed symmetrical bilayer composed of layers of the same composition is the sum of only two terms ($W_{\mathrm{RE}}+W_b$) [12], i.e., (a) the relative expansivity term

$$W_{\mathrm{RE}}=\frac{k_r}{2Ah^2}\,(\Delta A-\Delta A_0)^2, \tag{1}$$

where k_r is the nonlocal bending modulus, ΔA is the difference between the areas of the outer and the inner monolayers in the deformed state and is equal to $h\int(c_1+c_2)dA$, with c_1 and c_2 the principal curvatures and h the distance between the neutral surfaces of the outer and the inner monolayer, and ΔA_0 is the corresponding equilibrium area difference, and (b) the bending energy term

$$W_b=\frac{1}{2}k_c\int\,(c_1+c_2)^2dA, \tag{2}$$

where k_c is the bending modulus. The spontaneous curvature in the bending energy term [19] was taken to be zero because we are considering a symmetrical bilayer membrane. Also, we only consider vesicles with spherical topology and therefore the contribution of the Gaussian bending term to the bending energy is constant and is thus omitted.

The minima of elastic energy correspond to stationary shapes of the vesicle, so the problem is to find the extreme values of the membrane elastic energy. The shape of a flaccid vesicle is obtained from the minimum of $W_{\mathrm{RE}}+W_b$, where the membrane area is fixed. During the minimization procedure we also take into account that the volume of the vesicle (V) is fixed because of the incompressibility of water and the low water transmembrane transport. The constraints in volume and area can be incorporated in the energy minimization by introducing the Lagrange multipliers μ and λ, which represent the pressure difference across the membrane and the lateral tension. We wish to determine the axisymmetrical shape of a vesicle that is strained between two point forces acting in opposite directions at the vesicle poles. So the additional constraint that is important for the shape of the vesicle is the distance between the poles (Z_0). This distance can be kept constant by introducing the Lagrange multiplier f, which represents the axial force. Thus the shape equation for the vesicle is obtained by minimizing the functional

$$G=W_{\mathrm{RE}}+W_b-\mu V-\lambda A-fZ_0. \tag{3}$$

Because of recently debated controversies regarding the derivation of the shape equation for an axisymmetric vesicle (cf. [14,15,17,20]), the procedure for obtaining it from Eq. (3) is outlined in the following in some detail.

The expression for the membrane bending energy [Eq. (2)] for a given vesicle shape does not depend on the vesicle size. Due to this scale invariance, in the forthcoming minimization analysis the unit of length is chosen in such a way that the relative membrane area equals unity ($a=A/4\pi R_0^2=1$); thus $R_0=\sqrt{A/4\pi}$ is the radius of the sphere with the membrane area A. Then the relative vesicle volume is defined as $v=V/\frac{4}{3}\pi R_0^3$, the relative difference between the areas of the two membrane monolayers is defined as $\Delta a=\Delta A/8\pi hR_0$, where $8\pi hR_0$ is the relative difference between the areas of the two membrane monolayers for the sphere, and $z_0=Z_0/R_0$ is the distance between the poles in relative units.

It is also appropriate to measure the relative expansivity term, the membrane bending energy, and the functional G relative to the bending energy of the sphere ($8\pi k_c$): $w_{\mathrm{RE}}=W_{\mathrm{RE}}/8\pi k_c$, $w_b=W_b/8\pi k_c$, and $g=G/8\pi k_c$. Thus

$$w_{\mathrm{RE}}=\frac{k_r}{k_c}\,(\Delta a-\Delta a_0)^2, \tag{4}$$

where $\Delta a_0=\Delta A_0/8\pi hR_0$ is the equilibrium relative area difference. The functional [Eq. (3)] in the dimensionless form then reads

$$g=w_{\mathrm{RE}}+w_b-Mv-La-Fz_0, \tag{5}$$

where the new Lagrange multipliers M, L, and F are related to μ, λ, and f

$$M=\frac{R_0^3}{6k_c}\,\mu,\quad L=\frac{R_0^2}{2k_c}\,\lambda,\quad F=\frac{R_0}{8\pi k_c}\,f. \tag{6}$$

It is convenient to minimize the functional g separately with respect to Δa and for a given Δa with respect to the vesicle shape. The minimization of functional g with respect to Δa is performed as follows. At equilibrium the partial derivative of the functional g with respect to the relative area difference equals zero. This requirement leads to

$$\left.\frac{\partial(w_b+w_{\mathrm{RE}})}{\partial\Delta a}\right|_{\mathrm{eq}}=\left.\frac{\partial w_b}{\partial\Delta a}\right|_{\mathrm{eq}}+\left.\frac{dw_{\mathrm{RE}}}{d\Delta a}\right|_{\mathrm{eq}}=0, \tag{7}$$

where the fact that w_{RE} depends only on Δa is used. By considering the equation for the relative expansivity energy [Eq. (4)] one immediately obtains the equation

$$\left.\frac{\partial w_b}{\partial \Delta a}\right|_{\mathrm{eq}} = -2\frac{k_r}{k_c}(\Delta a - \Delta a_0), \tag{8}$$

which represents the condition for equilibrium. This equilibrium condition [Eq. (8)] is the same as for the case of no axial force [21,22].

The variation of the functional g with respect to the vesicle shape is performed by defining as a new variable N, the partial derivative of the relative bending energy with respect to the relative area difference ($N=\partial w_b/\partial \Delta a|_{\mathrm{eq}}$). From Eq. (7) it follows that N represents the relative lateral tension between the monolayers:

$$N = -\left.\frac{dw_{\mathrm{RE}}}{d\Delta a}\right|_{\mathrm{eq}}. \tag{9}$$

Because the relative expansivity term (w_{RE}) depends only on the relative area difference (Δa), the arbitrary variation of the relative expansivity term also depends only on the variation of the relative area difference ($\delta w_{\mathrm{RE}}=\delta\Delta a\, dw_{\mathrm{RE}}/d\Delta a|_{\mathrm{eq}}$). After using Eq. (9) the variation of the relative expansivity term (δw_{RE}) reads $-N\delta\Delta a$.

An axisymmetrical surface can be conveniently parametrized in relative units by the coordinates $r(s)$ and $z(s)$ [20], where r is the distance between the symmetry axis and a certain point on the contour, z is the position of this point along the symmetry axis, and s is the arclength along the contour. The angle of the contour $\psi(s)$ is defined through the equation $\tan\psi = dz/dr$, so the coordinates r and z depend on the angle ψ through the equations $\dot{r}=\cos\psi$ and $\dot{z}=\sin\psi$, where the overdot denotes the derivative with respect to the arclength s. The angle ψ and coordinate r are taken as two independent variables and the restriction for the geometrical relation between them is considered by a new Lagrange multiplier $\Gamma(s)$, which represents the component of the transverse shear force [11] in the radial direction. The variation of the functional y can then be expressed for an axisymmetrical vesicle as

$$\delta g = \delta\int_0^{s^*}\mathcal{L}\, ds, \tag{10}$$

where $\mathcal{L}$ is the Lagrange function

$$\mathcal{L} = \frac{r}{8}\left(\frac{\sin\psi}{r}+\dot{\psi}\right)^2 - M\,\frac{3r^2\sin\psi}{4} - L\,\frac{r}{2} - N\,\frac{\sin\psi+\dot{\psi}r}{4} - F\,\sin\psi + \Gamma(\dot{r}-\cos\psi) \tag{11}$$

and s^* is the length of the contour. The bending energy term in the functional [Eq. (10)] [$w_b=\frac{1}{8}\int_0^{s^*} r(\sin\psi/r+\dot{\psi})^2 ds$] includes the principal curvatures along the parallels ($\sin\psi/r$) and the meridians ($\dot{\psi}$). The geometrical parameters of the vesicle are given by integrals: $v=\frac{3}{4}\int_0^{s^*} r^2\sin\psi\, ds$ is the relative volume of the vesicle, $a=\frac{1}{2}\int_0^{s^*} r\, ds$ is the relative area of the vesicle, $\Delta a=\frac{1}{4}\int_0^{s^*} r(\sin\psi/r+\dot{\psi})ds$ is the relative area difference, and $z_0=\int_0^{s^*}\sin\psi\, ds$ is the distance between the poles, respectively.

Because the variation of the functional [Eq. (10)] with respect to all independent variables along the contour has to vanish ($\delta g=0$), one obtains differential equations

$$\ddot{\psi}r = \frac{\dot{r}\sin\psi}{r} - \dot{\psi}\dot{r} - 3Mr^2\cos\psi - 4F\cos\psi + 4\Gamma\sin\psi, \tag{12}$$

$$\dot{\Gamma} = \frac{1}{8}\left(\dot{\psi}^2 - \frac{\sin^2\psi}{r^2}\right) - \frac{3Mr\sin\psi}{2} - \frac{L}{2} - \frac{N\dot{\psi}}{4}, \tag{13}$$

$$\dot{r} = \cos\psi, \tag{14}$$

and conditions

$$H\delta s|_0^{s^*} = 0, \tag{15}$$

$$\frac{1}{4}(r\dot{\psi}+\sin\psi-Nr)\delta\psi|_0^{s^*} = 0, \tag{16}$$

$$\Gamma\,\delta r|_0^{s^*} = 0, \tag{17}$$

where

$$H = \frac{r}{8}\left(\dot{\psi}^2 - \frac{\sin^2\psi}{r^2}\right) + \frac{3Mr^2\sin\psi}{4} + \frac{Lr}{2} + \frac{N\sin\psi}{4} + \Gamma\cos\psi + F\sin\psi \tag{18}$$

is the Hamiltonian function. The contour of a vesicle is obtained by solving Eqs. (12)–(14). Equations (15)–(17) represent the boundary conditions that have to be fulfilled at the beginning ($s=0$) and at the end ($s=s^*$) of the contour [20]. Because the length (s^*) is not fixed ($\delta s|_{s^*}\neq 0$) and H is constant, Eq. (15) shows that $H=0$. Equation (16) shows that $\psi=0$ on the axis. This means that the vesicles are smooth at the poles. Because the coordinate r equals zero at the beginning and at the end of the contour [$r(0)=r(s^*)=0$], Eq. (17) is automatically fulfilled on the axis.

In order to solve the differential equations the behavior of the contour, i.e., the dependence of the angle ψ on r close to the symmetry axis, has to be investigated. For this it is convenient to eliminate Γ and s from the differential equations [20]. This is done by first rewriting Eq. (12) as $\Gamma=\Gamma(\ddot{\psi},\dot{\psi},\psi,r)$ and then inserting the expression obtained for Γ into expression (18) for $H=0$, which gives the equation of the contour in the form $\ddot{\psi}=\ddot{\psi}(\dot{\psi},\psi,r)$. Then the arclength s is eliminated by considering Eq. (14), and the shape equation appears in the form

$$\psi''\cos\psi - \psi'^2\sin\psi = \frac{r}{2\cos^2\psi}\left[\frac{\sin\psi}{r}\left(\frac{\sin^2\psi}{r^2} - \psi'^2\cos^2\psi\right) - 6M - 4L\,\frac{\sin\psi}{r} - 2N\,\frac{\sin^2\psi}{r^2} - 8F\,\frac{1}{r^2}\right] - \left(\frac{\psi'\cos\psi}{r} - \frac{\sin\psi}{r^2}\right), \tag{19}$$

where the prime denotes the derivative with respect to the coordinate r. [The same equation for $N=0$ was presented by

Zheng and Liu [23], who showed that Eq. (19) is also the first integral of the general shape equation [16] for the axisymmetrical case [15] with F an integration constant.] In the limit $r \to 0$ the solution of Eq. (19) has the form [14]

$$\psi = (-2F \ln r + B) r, \tag{20}$$

where B is a constant. In the absence of the axial force the constant B represents the value of the two principal curvatures on the vesicle poles [8]. In the procedure for obtaining the vesicle shape the values of M, L, N, F, and B are found to fulfill the conditions of the chosen v, a, Δa_0, and z_0 and to fulfill the condition that the transverse shear force (Γ) at the equator equals zero due to the mirror symmetry of the vesicle shape.

III. LIMITING SHAPES

The question of the maximal length of a vesicle with given volume, area, and area difference may be posed. In dimensionless representation, this means that we are looking for the shape with the extremal distance between the poles (z_0) under the conditions that the relative area (a) equals one and that the relative volume (v) and the relative area difference (Δa) are fixed. The maximal distance corresponds to an infinitely large axial force. We thus study the dimensionless functional

$$\tilde{g} = z_0 - \tilde{M} v - \tilde{L} a - \tilde{N} \Delta a, \tag{21}$$

where the Lagrange multipliers $\tilde{M}, \tilde{L}, \tilde{N}$ are

$$\tilde{M} = \frac{dz_0}{dv}, \quad \tilde{L} = \frac{dz_0}{da}, \quad \tilde{N} = \frac{dz_0}{d\Delta a}. \tag{22}$$

The functional $\tilde{g}$ can be expressed for an axisymmetrical vesicle as

$$\tilde{g} = \int_0^{s^*} \tilde{\mathcal{L}} \, ds, \tag{23}$$

where $\tilde{\mathcal{L}}$ is the Lagrange function

$$\tilde{\mathcal{L}} = \sin\psi - \tilde{M} \frac{3r^2 \sin\psi}{4} - \tilde{L} \frac{r}{2} - \tilde{N} \frac{\sin\psi + \dot{\psi} r}{4} + \tilde{\Gamma}(\dot{r} - \cos\psi). \tag{24}$$

The requirement for the geometrical relation between ψ in r is considered by the Lagrange multiplier $\tilde{\Gamma}$.

Because the variation of the functional [Eq. (23)] at equilibrium has to be zero, we obtain the equations

$$\cos\psi - \tfrac{3}{4} \tilde{M} r^2 \cos\psi + \tilde{\Gamma} \sin\psi = 0, \tag{25}$$

$$\dot{\tilde{\Gamma}} + \frac{3\tilde{M} r \sin\psi}{2} + \frac{\tilde{L}}{2} + \frac{\tilde{N} \dot{\psi}}{4} = 0, \tag{26}$$

$$\dot{r} = \cos\psi. \tag{27}$$

and the boundary conditions $\tilde{H} \delta s|_0^{s^*} = 0$, $(\tilde{N} r/4) \delta\psi|_0^{s^*} = 0$, and $\tilde{\Gamma} \delta r|_0^{s^*} = 0$, where

$$\tilde{H} = -\sin\psi + \frac{3\tilde{M} r^2 \sin\psi}{4} + \frac{\tilde{L} r}{2} + \frac{\tilde{N} \sin\psi}{4} + \tilde{\Gamma} \cos\psi \tag{28}$$

is the Hamiltonian function for this case. Because $\tilde{\mathcal{L}}$ does not explicitly depend on the arclength s, the Hamiltonian function is constant. Since the variation of $\tilde{g}$ with respect to variation of the contour length at the two end points must vanish, one obtains the condition $\tilde{H}(s^*) = 0$. Because the Hamiltonian function is constant along the contour, it follows that $\tilde{H} = 0$.

To simplify the numerical calculations, we can obtain an equation in a form without the Lagrange multiplier $\tilde{\Gamma}$. First Eq. (25) is rewritten as $\tilde{\Gamma} = \tilde{\Gamma}(\psi, r)$. This expression for $\tilde{\Gamma}$ gives, together with $\tilde{H} = 0$ [Eq. (28)],

$$3\tilde{M} r^2 + 2\tilde{L} r \sin\psi + \tilde{N} \sin^2\psi - 4 = 0. \tag{29}$$

The contour of a limiting vesicle is obtained by solving Eq. (29). On the poles, where $r = 0$, one obtains

$$\sin^2\psi_0 = \frac{4}{\tilde{N}}, \tag{30}$$

where ψ_0 is the angle of the contour on the symmetry axis. Equation (30) shows that the limiting vesicle shapes are not smooth at the poles and $\tilde{N}$ must be greater than or equal to 4 because there are no solutions that begin on the axis if $\tilde{N}$ is lower than 4. Equation (30) also shows that the contour of the limiting vesicle shape begins with the same angle ψ_0 on both poles. It can easily be seen from Eq. (25) that $\tilde{\Gamma}$ is zero on the equator, as it has to be because of the mirror symmetry of the limiting vesicle shapes.

IV. RESULTS

The results presented are restricted to vesicles belonging to a class of axisymmetrical prolate cigarlike shapes involving equatorial mirror symmetry. A systematic description of vesicle shapes under the effect of an axial force for other shape classes will be presented separately.

An increase in axial force in general causes an elongation of the vesicle and a change of the relative membrane area difference. Thus it is practical to represent vesicles of a given relative volume in a two-dimensional phase diagram as a function of the distance between the poles and the relative area difference (z_0-Δa phase diagram). In Fig. 1 the region of the z_0-Δa phase diagram is shown for a vesicle with a relative volume of 0.95 in the range of relative area differences where axisymmetrical prolate shapes with equatorial mirror symmetry exist in the absence of the axial force. Each point from this region is characterized by the corresponding Lagrange multipliers M, L, F and the relative lateral tension between the monolayers (N). The region is bounded from below by the curve (denoted by P) representing the lowest bending energy shapes of the prescribed symmetry when the axial force is equal to zero. These cigar class shapes exist within the interval of values of the area difference (Δa), where the shape with the smallest area difference is composed of a cylinder with two hemispherical caps (shape g in

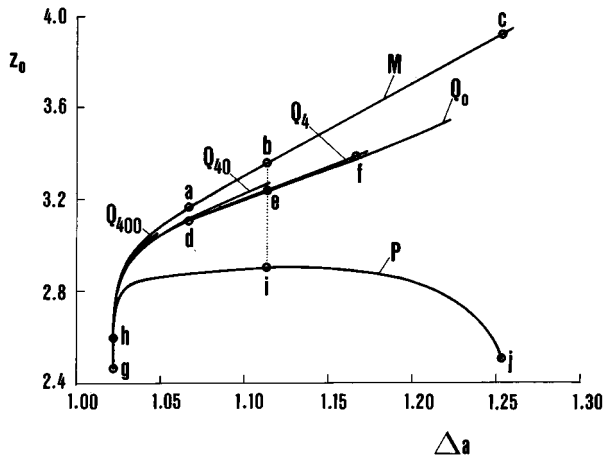

FIG. 1. The z_0-Δa phase diagram for prolate axisymmetrical shapes with equatorial mirror symmetry strained by an axial force for a vesicle with the relative volume $v=0.95$. The curve designated by P shows the dependence of the distance between the poles in relative units (z_0) on the relative area difference (Δa) for the prolate vesicles of the cigar class in the absence of the force. Some representatives of vesicles (denoted by g, h, i, and j) that belong to this curve are depicted in Fig. 2. The curve designated by M shows the dependence of the maximal distance between the poles on the relative area difference for the prolate vesicles. Some limiting shapes (denoted by g, a, b, and c) from this curve are depicted in Fig. 2. The dotted line is at $\Delta a_b=1.1134$. Curves designated by Q_0, Q_4, Q_{40}, and Q_{400} show the distance between the poles as a function of the relative area difference for the vesicles with the ratio between the nonlocal bending modulus and the bending modulus $k_r/k_c=0$, 4, 40, and 400. The curves Q_0, Q_4, Q_{40}, and Q_{400} are obtained by solving Eqs. (12)–(14) and (8) for different values of the axial force where the equilibrium area difference (Δa_0) is 1.0221. They begin on curve P (shape h), where $\Delta a=\Delta a_0$, and they end where numerical problems appear. Some examples of the shapes that are on the curve designated by Q_4 (denoted by d, e, and f) are depicted in Fig. 2.

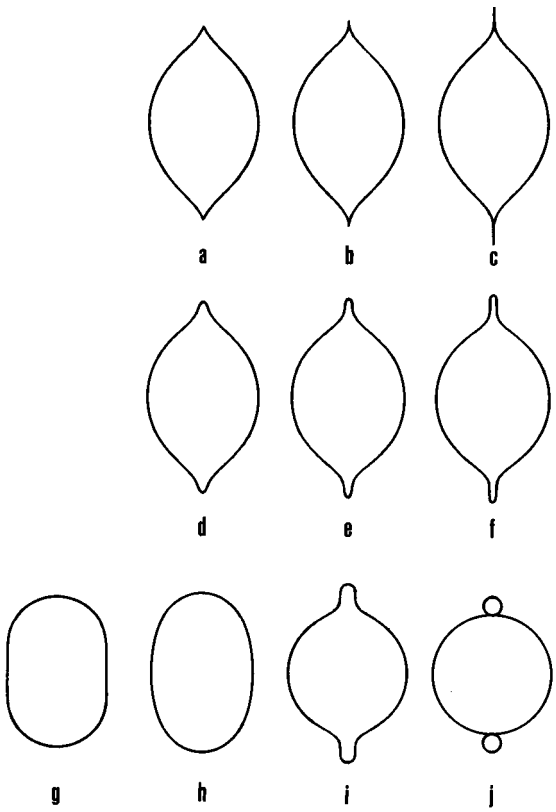

FIG. 2. Characteristic examples of axisymmetrical shapes with equatorial mirror symmetry at relative volume $v=0.95$. The position of each of these shapes in the z_0-Δa phase diagram is indicated in Fig. 1. The vesicle rotational symmetry axis is in the vertical direction. The shapes denoted by g, h, i, and j correspond to prolate vesicles of the cigar class in the absence of the force. The shapes denoted by d, e, and f are representatives of the vesicles that lie in Fig. 1 on the curve designated by Q_4. The contours of the vesicles denoted by d, e, f, g, h, i, and j are obtained by solving the system of differential equations [Eqs. (12)–(14)]. The parameters of these vesicles are given in Table I. The contours of the vesicles denoted by a, b, and c are obtained by solving Eq. (29) and the vesicles with these shapes are characterized in Table II. The shapes b, e, and i are at $\Delta a_b=1.1134$.

Fig. 2) and the shape with the largest area difference is the combination of one large and two small spheres (shape j). Two intermediate zero force shapes are also shown in Fig. 2 (shapes h and i). The shape denoted by h corresponds to the absolute minimum of bending energy. The parameters of these shapes are given in Table I. The curve M in Fig. 1 represents the shapes corresponding to an infinite force. For $v=0.95$ the infinite force shape at $\Delta a=1.0219$ coincides with the shape for $F=0$ (shape g), as this shape cannot be deformed. At higher Δa values the angle of the contour on the symmetry axis (ψ_0) increases (shape a), until at $\Delta a_b=1.1134$ it reaches the value $\pi/2$ (shape b) where $\tilde{N}$ equals 4 (Table II). The limiting shapes at higher Δa values differ from the shape at Δa_b by having on the axis on both sides an infinitesimally thin cylinder of length $2(\Delta a-\Delta a_b)$ (e.g., shape c). Namely, if $\tilde{N}=4$, the solution of Eq. (29) for the infinitely thin cylinder is

$$r=0, \quad \psi=\frac{\pi}{2}. \tag{31}$$

The infinitely thin cylinder has no volume and no area. It contributes only to the relative area difference and to the length of the limiting vesicle shape where $dz_0/d\Delta a=4$. The result presented can be considered as the upper limit (valid exactly for $h/R_0\rightarrow 0$) for the distance between the poles (z_0) at a given relative area difference (Δa) [24]. The parameters for different limiting shapes are given in Table II.

The limiting shapes (curve M) of vesicles represent the limit for an infinitely large axial force applied on the prolate vesicles (curve P) by keeping the relative area difference constant ($k_r/k_c=\infty$). As an example of the effect of the axial force one can note the shapes along the dotted line in Fig. 1 (shapes i, e, and b), which have the same area difference. It can be seen that the distance between the poles for these shapes increases on increasing the relative axial force. Shape e is similar to shape b except close to the poles.

For phospholipid vesicles the estimated ratio between the nonlocal and local bending moduli is finite [10] and therefore it is of interest to follow the vesicle shape changes by taking into consideration that the elastic energy is the sum of the

TABLE I. Properties of the vesicles that are presented in Fig. 2, where Δa is the relative area difference between the two membrane monolayers, z_0 is the distance between the poles in relative units, r_e is the relative radius of the vesicle on the equator, B is the parameter that denotes the behavior of the contour close to the pole [Eq. (20)], M is the relative pressure difference across the membrane, L is the relative lateral tension of the membrane, N is the relative lateral tension between the monolayers, and F is the axial force in relative units.

Shape	Δa	z_0	r_e	B	M	L	N	F
d	1.0670	3.106	0.908	−8.364	43.665	−68.917	−0.359	4.433
e	1.1134	3.240	0.918	−7.278	52.241	−81.560	−0.730	4.644
f	1.1668	3.387	0.926	−9.565	65.539	−101.497	−1.158	5.184
g	1.0219	2.465	0.811	1.233	$-\infty$	∞	$-\infty$	0
h	1.0221	2.593	0.829	1.490	−1.882	2.682	0	0
i	1.1134	2.901	0.973	9.078	9.558	−17.866	7.629	0
j	1.2535	2.507	0.981	7.348	20.7	−34.9	8.35	0

local and nonlocal bending terms [Eqs. (2) and (1)]. As an example we look for the effect of the axial force on the vesicle with the equilibrium relative area difference (Δa_0), corresponding to the shape *h* in Fig. 1, i.e., the shape with the absolute bending energy minimum in the case of a zero axial force. For this case the relative area difference equals the equilibrium relative area difference. Figure 1 shows the curves (Q_0, Q_4, Q_{40}, and Q_{400}) in the z_0-Δa phase diagram of shape changes due to the increase of axial force for four different values of the ratio k_r/k_c (0, 4, 40, and 400). Some examples of the corresponding shapes that lie on the curve for $k_r/k_c=4$ are also shown in Fig. 2 (shapes *h*, *d*, *e*, and *f*). The tubular endings at the poles of shapes *e* and *f* show the formation of tethers.

In Fig. 3 the dependence of the distance between the poles on the applied axial force when straining the vesicle with the initial shape *h* is presented. It can be noted that at smaller values of the ratio k_r/k_c there is a steep increase in the distance between the poles in the region of the shape changes where the vesicle begins to form the tether (i.e., from shape *d* to shape *e* for $k_r/k_c=4$). For the relative volume 0.95 at values where the ratio k_r/k_c is smaller than the critical ratio $(k_r/k_c)_c=1.89$, a discontinuous transition into tether conformation is predicted. The value of the critical axial force in relative units (F_c), which corresponds to this critical ratio, is equal to 4.47.

The value of the critical ratio between nonlocal and local bending moduli [$(k_r/k_c)_c$] and the value of the corresponding critical axial force (F_c) depend on the relative volume (Fig. 4). It may be seen from Fig. 4(a) that at higher relative volumes a discontinuous shape transition occurs at higher values of the ratio k_r/k_c. It can also be seen [Fig. 4(b)] that the critical axial force (F_c) increases with the relative volume. The dependence of $(k_r/k_c)_c$ on v shows that there is no discontinuous shape transition below a certain relative volume.

The Lagrange multipliers that represent the pressure difference across the membrane, the lateral tension, the relative lateral tension between the monolayers, and the axial force steeply increase when a tether is elongated. If the Lagrange multipliers are sufficiently large, an estimate of the relative radius of the tether (r_t) could be given, because on the section of the tether where $\psi\approx\pi/2$ the first derivative of the angle ψ with respect to the arclength s is almost zero ($\dot{\psi}\approx 0$). One obtains from Eq. (18)

$$-\frac{1}{8r_t}+\frac{3Mr_t^2}{4}+\frac{Lr_t}{2}+\frac{N}{4}+F=0 \tag{32}$$

and from Eq. (13)

$$\frac{1}{8r_t^2}+\frac{3Mr_t}{2}+\frac{L}{2}=0. \tag{33}$$

After eliminating L from Eqs. (32) and (33) we have

$$-3Mr_t^3-1+Nr_t+4Fr_t=0. \tag{34}$$

For the shape denoted by *e* the product $3Mr_t^3$ is equal to 0.039, the product Nr_t is equal to -0.046, and the product $4Fr_t$ is equal to 1.17. The product Mr_t^3 decreases with increasing relative axial force for the vesicle with the certain ratio k_r/k_c. Because for the elongated tether the product Mr_t^3 is much smaller than Nr_t+4Fr_t-1, after using Eq. (8) the radius of the tether ($R_t=R_0r_t$) can be approximated in dimensional form by the equation

TABLE II. Properties of the limiting vesicles that are presented in Fig. 2, where Δa is the relative area difference between the two membrane monolayers, z_0 is the distance between the poles in relative units, r_e is the relative radius of the vesicle on the equator, and ψ_0 is the angle of the contour on the poles. The Lagrange multipliers $\tilde{M},\tilde{L},\tilde{N}$ are defined through Eqs. (22).

Shape	Δa	z_0	r_e	ψ_0	$\tilde{M}$	$\tilde{L}$	$\tilde{N}$
a	1.0670	3.166	0.895	1.243	−6.486	8.444	4.463
b	1.1134	3.357	0.898	$\pi/2$	−7.050	9.498	4
c	1.2535	3.917	0.898	$\pi/2$	−7.050	9.498	4
g	1.0219	2.465	0.811	0	∞	$-\infty$	∞

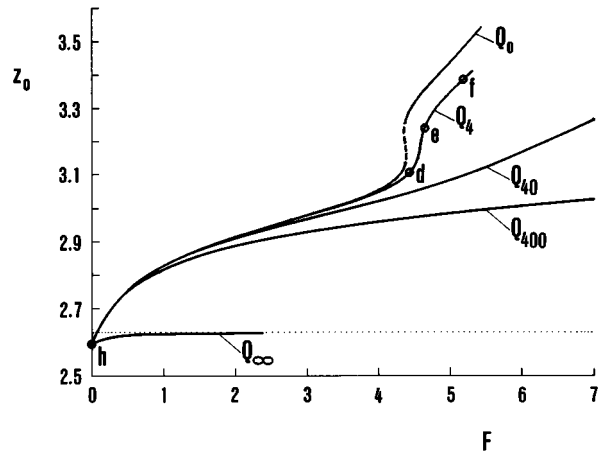

FIG. 3. Distance between the poles in relative units (z_0) as a function of the relative axial force (F) where the curves designated by Q_0, Q_4, Q_{40}, Q_{400}, and Q_∞ show the dependences for five different values of the ratio between the nonlocal and local bending moduli ($k_r/k_c=0$, 4, 40, 400, and ∞). The equilibrium relative area difference of the two membrane monolayers (Δa_0) is 1.0221. The curves for $k_r/k_c=0$, 4, and 40 are the most inclined close to $z_0=3.2$, where the tether appears. The letters h, d, e, and f indicate the positions of the vesicle shapes that are depicted in Fig. 2. For $k_r/k_c=\infty$ (curve designated by Q_∞) the maximal distance between the poles exists at $z_0=2.630$ (dotted line).

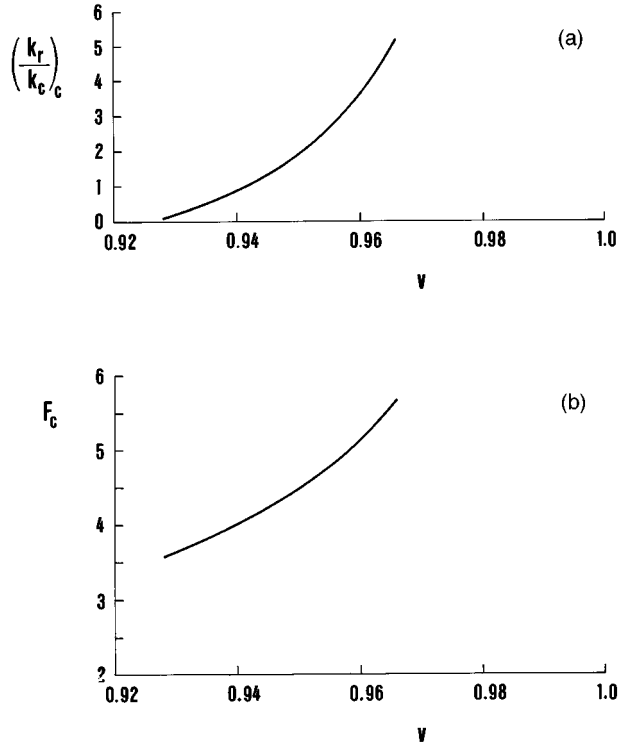

FIG. 4. (a) Dependence of the critical ratio between the elastic constants $[(k_r/k_c)_c]$ on the relative vesicle volume (v). There is a discontinuous transition in vesicle shape for the vesicles that lie below the curve. The curve ends at relative volume 0.966, where numerical problems appear. (b) Corresponding dependence of the critical axial force (F_c).

$$\frac{2\pi k_c}{R_t}+\frac{2\pi k_r(\Delta A-\Delta A_0)}{Ah}-f=0. \tag{35}$$

This equation predicts the same radius for the tether as the equation for the tether equilibrium of the simple geometrical model (Eq. 21 of Ref. [12]).

V. DISCUSSION

The variety of vesicle shapes obtained under the conditions of the applied axial force is discussed first in relation to the variety of shapes of freely suspended flaccid phospholipid vesicles or structurally related cells. A large variety of shapes within different symmetry classes has already been found in the latter case [7,8,25]. Under the influence of the external axial force the shape variety greatly increases. A demonstration of this is the phase diagram for the class of prolate axisymmetrical shapes exhibiting equatorial mirror symmetry, as a function of distance between the vesicle poles and the area difference presented in Fig. 1. In this phase diagram the shapes for the case of zero force are points on a curve (curve P), whereas the shapes under applied axial forces correspond to the points within a certain area of the z_0-Δa phase diagram bounded on two sides by the curves P and M. In both cases the shapes are solutions of the generalized shape equation [16]; however, these solutions differ in their behavior at the poles. In the case of a nonzero force the principal curvatures at the poles depend logarithmically on the distance from the axis [see [14] and Eq. (20)], whereas in the case of a freely suspended vesicle the shape behavior in the poles is normal, giving rise to the requirement that the two principal curvatures are always finite and equal [8]. The different extent of the shape variety can thus be directly related to the different restrictions in the boundary condition on the axis.

By following up the shape transformations under the effect of the axial force it is possible to envisage why tethers are formed. The vesicle shapes under the effect of the axial force are governed, on the one hand, by the tendency of the system to be as elongated as possible and, on the other hand, by the opposing tendencies due to the constraints on the constant vesicle area and volume. The dependence of the distance between the poles on the axial force determined for a reasonable value of the ratio between the bending moduli (curve Q_4 in Fig. 3) reveals two regimes with regard to the response of the vesicle to the axial force. At relatively low values of the force (before reaching shape d) a vesicle can adjust to the strain by changing its shape over its whole surface, whereas at larger forces (after reaching shape e) the vesicle can further adapt only by forming tethers, by which the distance between the poles can increase the most by taking into the tethers the minimum possible amount of the vesicle interior and membrane area. A tether is an almost cylindrical section of the vesicle where the distance between the membrane and the symmetry axis is practically constant.

After a tetherlike conformation is established, a further increase of axial force causes elongation of the tethers and a decrease in their radii [Eq. (34)]. The longer the tethers, the more membrane material than water drawn from the main vesicle body to such thin tethers. Thus, for a large axial force

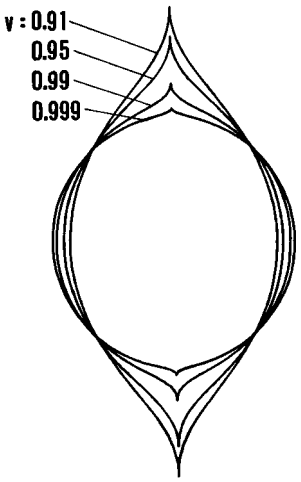

FIG. 5. Examples of the limiting shapes b for the different relative volumes $v=0.91$, 0.95, 0.99, and 0.999. These shapes correspond to the limiting vesicle shapes of the main vesicle body at infinitely large axial force. The rotational symmetry axis is in the vertical direction. The contours of the main vesicle bodies are obtained by solving Eq. (29) for $\tilde{N}=4$.

the pressure difference across the membrane, the lateral tension, and the relative lateral tension between the monolayers increase very much. Because the Lagrange multipliers F, M, L, and N steeply increase, the solutions of the differential equation for the vesicle shapes [Eq. (19)] in the limit $F,M,L,N\rightarrow\infty$ correspond to solutions of the differential equation for the limiting vesicle shapes [Eq. (29)], and the shape of the vesicle can be determined by integrating this equation. Consequently, the shape of the main body of a vesicle is expected to become similar to the limiting shape b (Figs. 1 and 2) throughout the whole region of space where tethers are formed. This notion can be visualized by comparing shapes e and b in Fig. 2. However, at larger tether lengths, the tether fraction of the membrane area may become significant relative to the total membrane area, meaning that effectively the shape of the main body would tend to assume the shape b corresponding to a higher relative volume. The limiting shapes b for different relative volumes are shown in Fig. 5. It can be visualized that at high enough tether lengths the shape of the vesicle main body would attain a spherical aspect. The radius of the vesicle on the equator increases on increasing the axial force (cf. shapes e and f in Table II). At an infinitely large axial force the radius of the main vesicle body on the equator is equal to the radius on the equator of the corresponding shape b.

For a large axial force the relative area difference is proportional to the distance between the poles since the contribution of the membrane on the tether section to the area difference depends only on the tether length. Because at large axial forces there are only slight changes in the shape of the main vesicle body, also the membrane area difference of the main vesicle body and the length of the main vesicle body are almost constant. Thus, when the distance between the poles increases by the lengthening of the tethers, the total area difference is proportional to the distance between the poles. The derivative of the relative area difference with respect to distance between the poles in relative units equals $\frac{1}{4}$. The value of this derivative, which is the same as for the limiting vesicle shape with infinitely thin tethers (curve M in Fig. 1 for $\Delta a>\Delta a_b$), does not depend on the ratio k_r/k_c. This means that at large axial forces the lines that represent the dependence of the distance between the poles on the relative area difference for different ratios k_r/k_c are parallel to the line of the corresponding dependence for the limiting shape. The higher the ratio k_r/k_c, the closer the line for the dependence of the distance between the poles on the relative area difference to the line for the corresponding dependence of the limiting shape. For any finite ratio k_r/k_c the limiting shape with infinitely thin tethers is never reached because the bending energy of such tethers is infinitely large.

When tether conformation is established, vesicle lengthening is essentially resisted by the contributions to the elastic energy of the tether sections of the vesicle. This was a basic assumption in the approximate analysis of the tether pulling experiment [12,10,11], where the shape of the tether was approximated by a cylinder. The present analysis shows that the magnitudes of the axial forces are related to the tether radius in the same manner [Eq. (35)] as was already predicted on the basis of simple tether models [12]. This result thus justifies the use of simple geometrical tether models in the analysis of equilibrium tether experiments.

In this work the question of the stability of the calculated shapes of the treated shape class was not addressed systematically. It was tacitly assumed that the shapes calculated at given relative volume, relative area difference, and distance between the poles are the lowest-energy shapes of the treated symmetry, which is a generalization of the case of zero external force. The problem of stability is a relevant problem in view of the fact that in the case of zero force the cigar class shapes for Δa values larger than 1.0222 are unstable, having larger energies than the shapes with no equatorial mirror symmetry [25,26]. However, at least some of the shapes with mirror equatorial symmetry are also relevant at nonzero force, which is substantiated by observations of axially strained vesicles [18]. It is to be pointed out that the present analysis revealed a different type of instability within the treated class, i.e., the regions of instability at smaller ratios of k_r/k_c, as evidenced by the result presented in Fig. 3.

The material constant that essentially affects the behavior of axially strained phospholipid vesicles appears to be the ratio between the nonlocal and local bending constants k_r/k_c. The ratio k_r/k_c depends on the sort of lipid and on the number of layers in the membrane. The ratio k_r/k_c obtained for a mixture of 1-stearoyl-2-oleoyl-phosphatidylcholine and 1-palmitoyl-2-oleoyl-phosphatidylserine was approximately 3 [10]. This value applies to unilamellar membranes. For multilamellar phospholipid vesicles the ratio k_r/k_c can be considerably larger than for a bilayer [27].

At sufficiently low values of the ratio k_r/k_c a definite change into the tether regime occurs in a small interval of forces (Fig. 3). It is of particular interest that there is a discontinuous transition of the shape from the pretether to the tether conformation below the critical ratio of k_r/k_c, which is of the same order of magnitude as the measured value [10]. The critical ratio k_r/k_c is smaller for smaller relative volumes (Fig. 4) meaning that more flaccid vesicles can

adapt to the force by shape changes over their whole surface more easily. The critical ratio k_r/k_c increases with increasing relative volume of the vesicle, but also the corresponding relative forces at which the discontinuous transitions occur are larger. The predicted dependence of the critical ratio k_r/k_c on relative volume could provide a sensitive method for the determination of this material parameter, consisting of measuring the dependence of the vesicle length on the force at different relative vesicle volumes. For instance, from the results presented in Fig. 4 for the ratio $k_r/k_c=4$, the discontinuous transition of the vesicle shape is expected at relative volumes larger than 0.962. The relative volume at which the discontinuities in this dependence appear would provide for the ratio k_r/k_c, whereas from the corresponding force one could determine k_c.

The results presented may have relevance in some cellular processes. The force exerted by a single kinesin molecule is approximately 5 pN [28]. The forces needed for pulling the tether are of the same order of magnitude, which indicates that the formation of tubular cellular systems may actually be the natural consequence of the forces exerted by cytoskeletal systems. An estimation for the minimal force needed for formation of a tether can be given from the value of the product Fr_t for the shape denoted by e (Fig. 2), where the microtubes appear. Because for this shape the value for the product $4Fr_t$ is approximately 1, the force needed for tether formation can be given by the equation in dimensional form $f=2\pi k_c/R_t$. For $k_c\approx 10^{-19}$ J the radius of the tether, for forces (f) between 25 and 5 pN, ranges between 30 and 150 nm.

[1] N. Benlimame, D. Simard, and I. R. Nabi, J. Cell Biol. **129**, 459 (1995).

[2] S. L. Dabora and M. P. Sheetz, Cell **54**, 27 (1988); R. D. Vale and H. Hotani, J. Cell Biol. **107**, 2233 (1988).

[3] J. Dai and M. P. Sheetz, Biophys. J. **68**, 988 (1995).

[4] R. M. Hochmuth, N. Mohandas, and P. L. Blackshear, Jr., Biophys. J. **13**, 747 (1973).

[5] R. E. Waugh and R. G. Bauserman, Ann. Biomed. Eng. **23**, 308 (1995).

[6] R. E. Waugh, Biophys. J. **38**, 29 (1982).

[7] H. J. Deuling and W. Helfrich, J. Phys. (Paris) **37**, 1335 (1976).

[8] S. Svetina and B. Žekš, Eur. Biophys. J. **17**, 101 (1989).

[9] L. Bo and R. E. Waugh, Biophys. J. **55**, 509 (1989).

[10] R. E. Waugh, J. Song, S. Svetina, and B. Žekš, Biophys. J. **61**, 974 (1992).

[11] E. Evans and A. Yeung, Chem. Phys. Lipids **73**, 39 (1994).

[12] B. Božič, S. Svetina, B. Žekš, and R. E. Waugh, Biophys. J. **61**, 963 (1992).

[13] S. Svetina and B. Žekš, in *Nonmedical Applications of Liposomes*, edited by D. D. Lasic and Y. Barenholz (CRC, Boca Raton, FL, 1996), p. 13.

[14] R. Podgornik, S. Svetina, and B. Žekš, Phys. Rev. E **51**, 544 (1995).

[15] Hu Jian-Guo and Ou-Yang Zhong-Can, Phys. Rev. E **47**, 461 (1993).

[16] Ou-Yang Zhong-Can and W. Helfrich, Phys. Rev. A **39**, 5280 (1989).

[17] H. Naito and M. Okuda, Phys. Rev. E **48**, 2304 (1993); H. Naito, M. Okuda, and Ou-Yang Zhong-Can, Phys. Rev. Lett. **74**, 4345 (1995).

[18] H. Hotani and H. Miyamoto, Adv. Biophys. **26**, 135 (1990); M. Elbaum, D. K. Fygenson, and A. Libchaber, Phys. Rev. Lett. **76**, 4078 (1996).

[19] W. Helfrich, Z. Naturforsch. Teil C **28**, 693 (1973).

[20] F. Jülicher and U. Seifert, Phys. Rev. E **49**, 4728 (1994).

[21] V. Heinrich, S. Svetina, and B. Žekš, Phys. Rev. E **48**, 3112 (1993).

[22] M. Jarić, U. Seifert, W. Wintz, and M. Wortis, Phys. Rev. E **52**, 6623 (1995).

[23] Wei-Mou Zheng and Jixing Liu, Phys. Rev. E **48**, 2856 (1993).

[24] The length of the infinitely thin cylinder also represents a good estimate for thin enough membrane tubes. For instance, the distances between the poles in relative units (z_0) obtained for a vesicle with $R_0=10$ μm, $h=2.5$ nm, $v=0.95$, and a cylinder of radius $10h$ differ from distances z_0 obtained for the vesicle with an infinitely thin cylinder by less than 2×10^{-3} of their values in the range of Δa between Δa_b and the relative area difference of the shape c (1.2535).

[25] U. Seifert, K. Berndl, and R. Lipowsky, Phys. Rev. A **44**, 1182 (1991).

[26] S. Svetina and B. Žekš, J. Theor. Biol. **146**, 115 (1990).

[27] S. Svetina and B. Žekš, Eur. Biophys. J. **21**, 251 (1992).

[28] K. Svoboda and S. M. Block, Cell **77**, 773 (1994).